CHAPTER-4

CHRONOLOGY OF LACUSTRINE SEDIMENTS IN CENTRAL HIMALAYA

Garbayang

Heim and Gansser (1939) were the first to report extensive glacio-lacustrine deposits at Garbayang in the Kali River basin bordering Tibet (Fig. 4.1). These deposits are spread over 0.05 sq km in a NE-SW trending valley drained by the river Kali that enters the basin from the north and flows southwest. The Chhiyalekh (Lekh=mountain pass, 3100m) in the SW acts as a major structural divide and demarcates the southern limit of the basin The total thickness of relict lake sediments is ~ 100 m However, the present study is confined to the upper ~29 m. Sedimentary architecture and textural attributes of the sediments indicate a deposition under proglacial lacustrine environment. Field evidence suggests that lake formed after the retreat of the main valley glacier that deposited its terminal moraine and blocked a narrow gorge at the base of the Chhiyalekh.

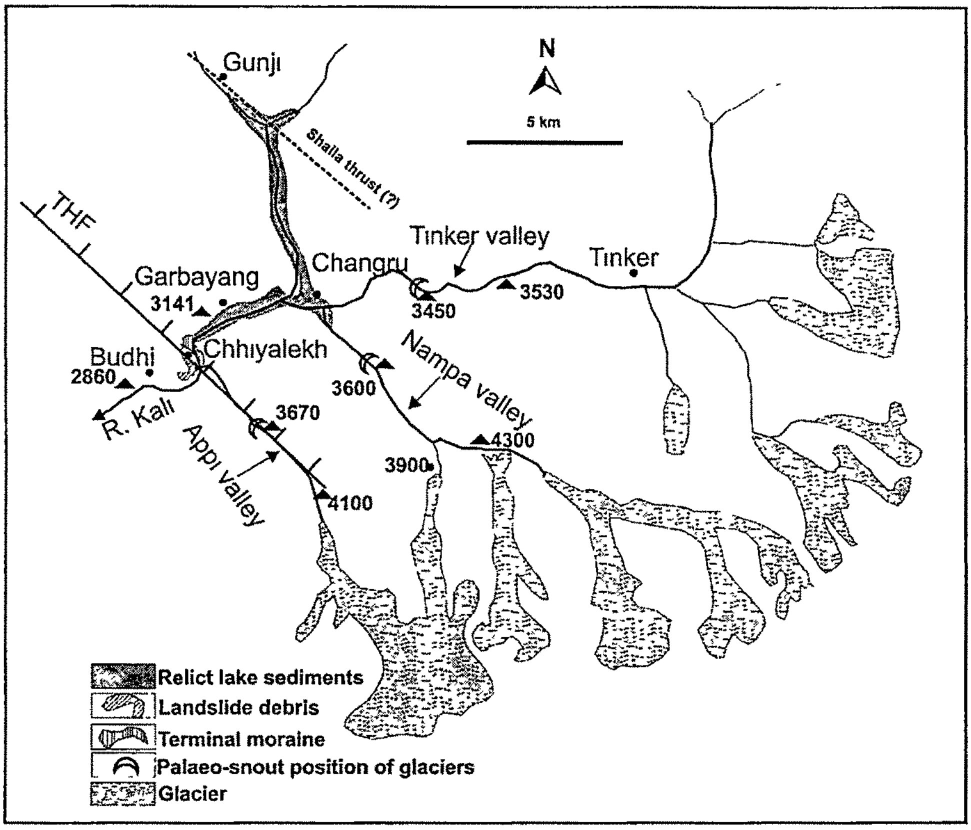

Figure-4.1. Geomorphological map of Garbayang basin. Dark shaded area along Kali river show the extent of proglacial lake deposits (modified after Heim and Gansser, 1939).

The varve/rhythmites sedimentation that commenced after the formation of this lake, ceased with the deposition of the outwash gravel. This event caused draining off the lake and exposed an extensive flat ground for habitation.

The above field observations raised a few pertinent questions, e.g (i) what determined the geomorphologic evolution of Garbayang basin during late Quaternary? (ii) what was the pattern of lacustrine sedimentation and the amplitude and timing of climatic and seismic events?

Geology and geomorphology

Trans Himadri Fault (THF) an equivalent of the South-Tibetan Detachment Systems (STDS) separates rocks of Garbayang Formation (Tethyan Zone) in the north from the Central Crystalline dominated by Precambrian biotite-porphyroblast schist (the Budhi schist) in the south (Fig. 4.2, Gansser, 1964; Valdiya, 1987, 1993). The basal Garbayang Formation (named after the Garbayang village) has been assigned an early Cambrian-to- Late Cambrian age and is dominated by alternating bands of calcilutite calcsilicate and brown dolomitic limestone. This is followed by crinoidal and oolitic limestone in the middle and cross-bedded calcareous sandstone (calcsilicate) and alternating bands of sandstone and shale in the upper part (Shah and Sinha, 1975). The rocks north of Garbayang basin belong to fossiliferous Shiala Formation of Ordovician age and comprise variegated shales with sandy limestone and crinoidal breccias. (Gansser, 1964; Valdiya, 1987). In the vicinity of the relict lake deposits calcsilicate, quartzite and shale dominate the lithology (Fig. 4.2).

Garbayang basin that lies north of 3100 m Chhiyalekh ridge is a topographical expression of the THF that opens into an almost flat terrain towards the north. The basin is flanked by steep slopes with snow clad Appi and Nampa valley that rise above 7000 m and support massive glaciers on left flank of the basin in the Nepalese territory (Fig. 4.1). On the right flank, the peaks seldom rise above 5000 m and have fewer glaciers.

Heim and Gansser (1939) observed three generations of moraines deposited by the retreating glaciers, at 3600m, 4050m, and 4400m altitude along Appi and Nampa valleys. They further observed Garbayang lake deposit to transgress over the 'lowest and biggest' (oldest) moraines in the basin indicating that the Garbayang lake formed after the 'biggest' moraine blocked river Kali at the base of Chhiyalekh (Fig. 4.1). Subsequent glacial advances were of a lesser extent. Similar evidence accrues from other river basins, viz. the Gori Ganga and the Dhauli Ganga where the terminal moraines of the earliest glacial advance stop at ~3000 m terminate against the THF impounding the rivers at places (Fig. 4 2)

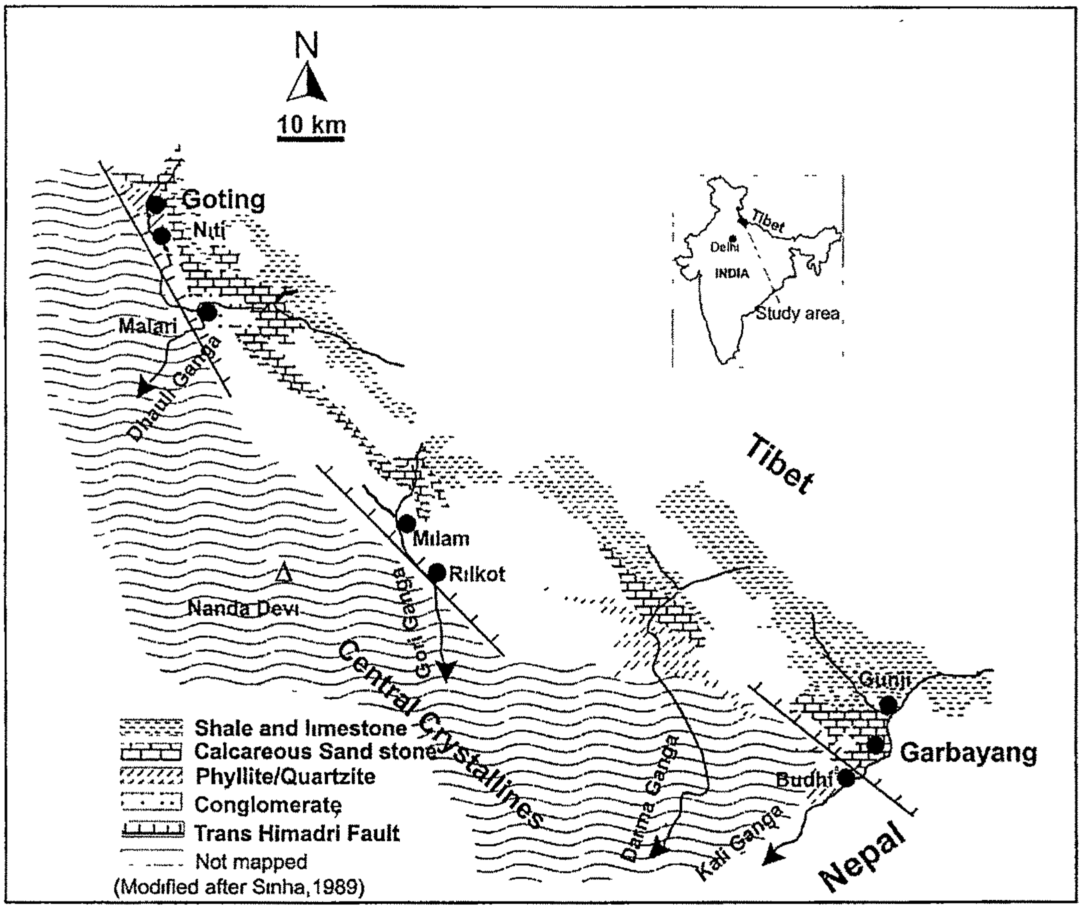

Figure-4.2. Lithology and structure in the study area.

The sedimentation pattern that followed after the deposition of basal moraines indicates calm water condition characterized by mm scale planar structures comprising alternating dark and light streaks. The sedimentary structure of the beds and the proximity of terminal moraines of the succeeding advance at ~3600 m altitude suggests that deposition took place in a proglacial lacustrine environment (Fig. 4 1). However, occasional presence of sand layers, thick carbonaceous laminae, faulted strata and occasional dropstones suggested that deposition was not altogether monotonous. The entire lacustrine succession is capped by a ~3 m thick outwash gravel (Fig. 4.3). This is the time when the lake breached and the river Kali drained out through a narrow gorge at the base of Chhiyalekh. Subsequently, various 'nallahs' (gullies) and avalanche chutes dissected the entire landscape. In addition, the torrents of river Kali have since been constantly eroding the toe of vertical cliffs that sculpted an otherwise flat surface into various steps analogous to the creation of bergschrunds in glaciers and in the loess landscape. Massive landslide debris at the tectonic contact between the Budhi schist and Garbayang Formation can be observed on top of Chhiyalekh ridge (Fig. 4.1) where river Kali has cuts a deep gorge.

Sedimentology of lacustrine deposits

Out of ~100 m of sediment succession at Grabayang, upper 29 m of an undisturbed location in the central part of the basin was measured and sampled (Fig. 4.3). Sections attached to the steep valley walls that form the lake margin were not sampled to minimize complication arising from sliding, slumping and inclusion of extraneous debris. Care was taken to ensure stratigraphic continuity wherever faulted strata occurred. Figure 4.3 summarizes the stratigraphy of the upper part of the lake deposits.

Physical characteristics

In a freshly exposed section the beds appear as stacked bundles of thin horizontal streaks of variable thickness ranging from mm to cm scale. Closer examination of the layers revealed that individual units comprised a couplet of dark and a light-coloured band of fine silty-clay (Fig. 4.4A) The light coloured streaks had a lime powdery texture and the dark bands contained organic debris. At places, prominent black coloured or yellow rust coloured streaks intercalated the succession. Another characteristic feature was the occurrence of 'dropstones' of varying sizes. The largest dropstone seen was 10 cm across the horizontal axis. It was found laying flat, compressing the planar beds to bend downwards under its weight. The overlying laminae followed the surface contour of the dropstone (Fig. 4.4B). At places thick (~5 cm) organic rich layers interspersed the sequence (especially in the middle part of the succession).

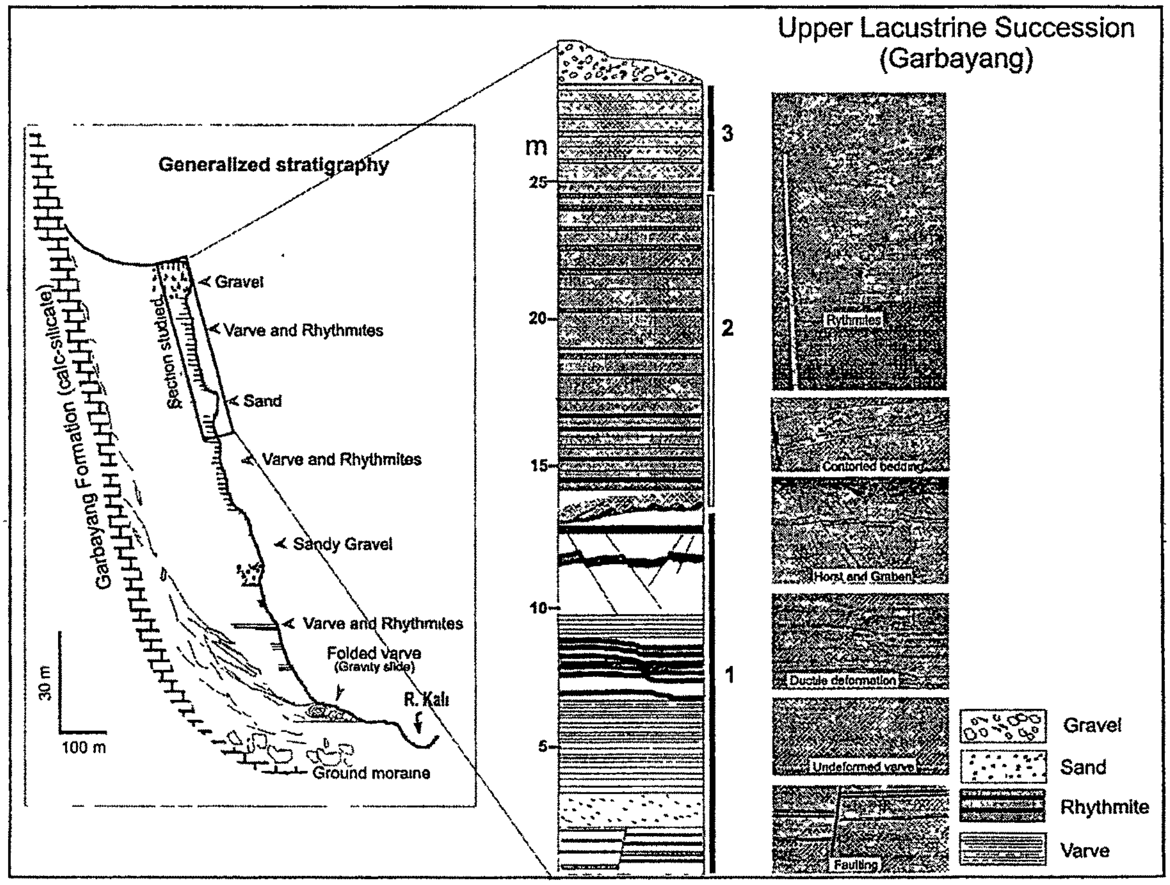

Figure-4.3. Stratigraphy of the upper lacustrine succession, inset is the composite stratigraphy. Representative field photographs are shown alongside the log.

Petrography

Petrology of the varves was carried out to reconstruct the depositional environment and its seasonal variability. Sharp contact between the seasonal layers was observed under the microscope. Two superimposed contrasting bands, the upper greyish brown fine clay (dark band) and the lower greyish yellow (light band) fine silt (Fig. 4.4C) were seen. The matrix showed calcareous cement with concordant calcareous laminae. The silt laminae contained quartz and calcite that are embedded in calcareous matrix. Calcareous silt showed microsparite and disoriented mica flakes. The dark coloured lamina additionally contained thick clouds of organic debris.

Physical stratigraphy

The sedimentary architecture and textural attributes of the laminations enabled three-fold sub-division of the upper lacustrine succession (Fig. 4.3)

Unit-1 Measured bottom upward the lower part of the profile (0-13.40 m) had a consistent varve succession of planar laminar beds typically 0.2 cm to 0.5 cm thick. Each lamina comprised thin alternating dark and light colour streaks. A 1.70 m thick sand body punctuated the varve sedimentation. A thick (~7 cm) dark sticky mud deposit towards the upper part of the Unit-1 (13.40 m) indicated temporary hiatus in the varve sedimentation (Fig. 4.3). Three faulting events separated by planar beds occur between 0-13 m (Fig. 4.3)

Unit-2 This unit which overlies Unit-1 continues from 13.40 m - 24 m. and is dominated by dark coloured planar sticky muds that frequently intercalated the

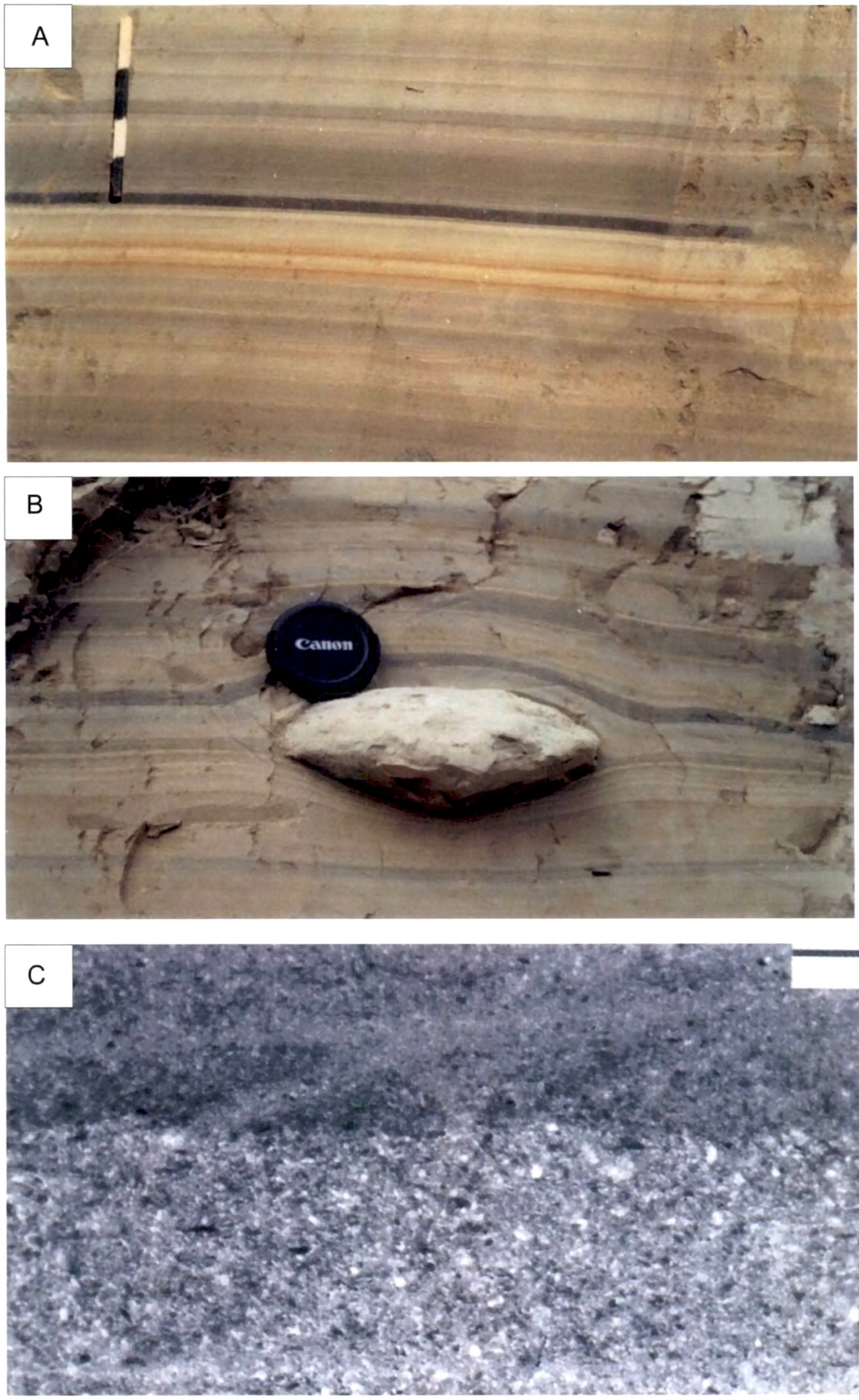

Fig 4.4. A Typical varve laminae (scale 4cm).
B Drop stone embedded in varve.
C Thin section of individual varve lamina showing dark winter layer and light summer layer (12 micron).

varves The thickest mud horizon measured 7 cm. The varves become thicker in the middle part of this unit with thickness varying from 0.5 cm to 3 cm, however, the grain size of the individual layers remained similar to that of varve dominated Unit-1.

Unit-3. This unit between 24.0 m – 28.40 m was characterized by three distinct features; (i) less frequent carbonaceous bands with decreasing organic carbon content (imparting brownish grey hue to the laminations) (ii) broken laminae in the upper part of the succession and (iii) an increase in the calcium carbonate and sandy-silt contents towards the top.

Sedimentation process

The pattern of sedimentation was typical of proglacial lacustrine environment. In such environment, the lakes are thermally stratified during the summer with warm water in the upper part (epilimnion) and colder water in the lower part (hypolimnion). The upper warm layer remains in exchange with the atmosphere. A cold glacial melt water with suspended sediments gives rise to heavy density current flow during summer and deposited at the lake bottom as underflow (Fig. 4.5A). These layers are light coloured and relatively coarse grained. During winters, meltwater and the autochthonous sediment supply decreases, thermal stratification disappears and the lake becomes well mixed (Fig. 4.5B). Stokes sedimentation of the fine suspended particles then take place. Besides this, freezing of the surface water cuts off any exchange between lake water and the atmosphere.

Consequently, available dissolved oxygen is gradually depleted at the expense of CO_2 thereby enhancing the preservation of organic content as dark, very fine-grained lamina. Occurrence of dropstones- a diamictic lithology produced by ice rafting in

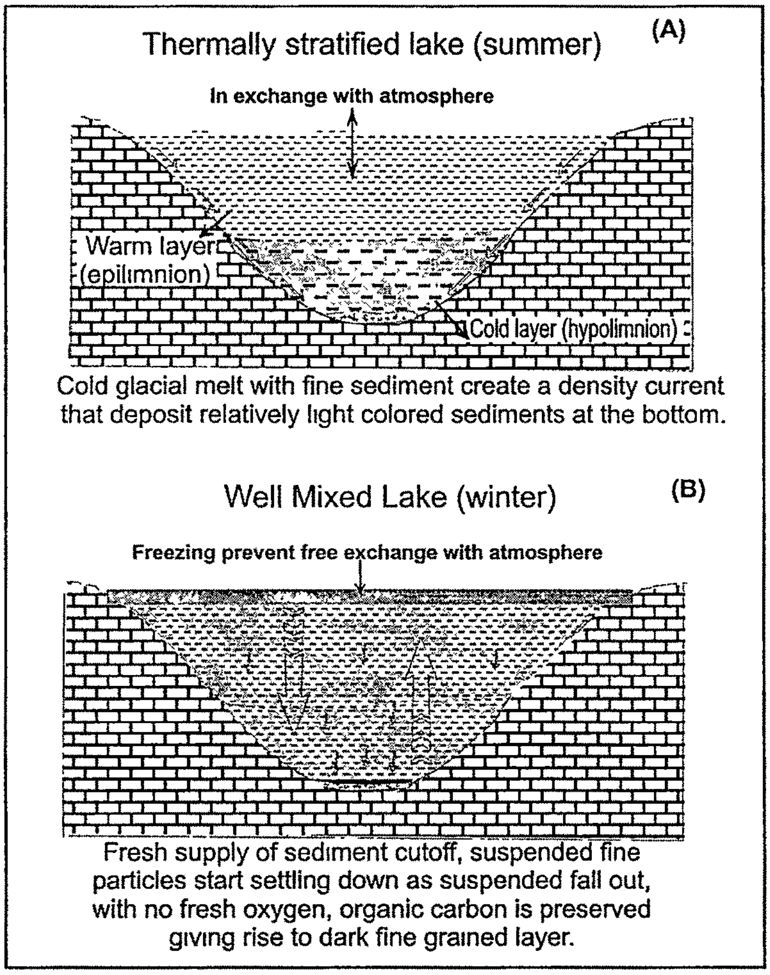

Figure 4.5 Based on Geyh et al., 1998.

suspension that deposits on the lake bottom. The situation implies breaking of ice front that requires marginal rise in the ambient temperature. Since sedimentary succession is dominated by varves and rhythmite and does not show any significant compositional variation, it suggests that conditions during their deposition should have remained essentially glacial.

Magnetic susceptibility and magnetomineralogical S-ratio

Catchment lithology, more specifically the primary magnetic mineral content determines the overall type and concentration of magnetic minerals in lake sediments

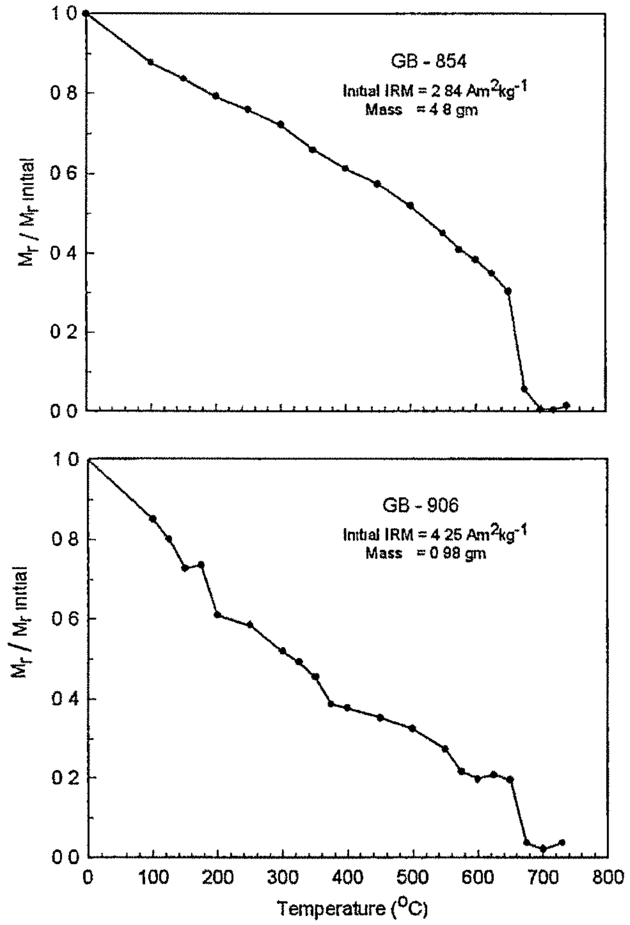

Figure-4.6. Stepwise thermal demagnetization of the normalized IRM values. Sample GB-854 indicate dominance of Hematite (curie temperature ~675 – 700 ^{0}C) and sample GB-906 contain Titanium bearing magnetite (curie temperature 200, 400 and 580 ^{0}C).

(Oldfield et al., 1983). To delineate changes in magnetic mineralogy of the sediments, magnetic susceptibility (χ) and magnetomineralogical S-ratio, Isothermal Remanent Magnetisation (IRM)/Saturation Isothermal Remanent Magnetisation (SIRM), simplified here as $IRM_{-300mT}/SIRM_{1\ 5T}$ were used. Variation in χ indicates changing concentration of magnetic minerals while the S-ratio provide a measure of the relative proportions of higher coercivity magnetic minerals (hematite) to lower coercivity magnetic mineral (magnetite). A total of 1175 samples collected at 2 cm interval were analyzed for magnetic susceptibility and S-ratio. To further characterize magnetic mineralogy of the sediments, few samples were also analyzed by thermal demagnetization and SIRM using a MMTD60 Furnace (Magnetic Measurements) (Fig. 4.6).

Relatively high values of magnetic susceptibility and S-ratio indicate a close relationship between the erosional processes and increasing detrital titanomagnetite concentration (Williamson et al., 1998). It has been suggested that fluctuation of χ in lacustrine sediments is modulated by the climate (Verosub and Roberts, 1995). However, a direct climatic connection needs consideration on the influence of changes in lake chemistry that is modulated by fluctuating fresh water influx and has strong influence on the type and concentration of magnetic mineralogy (Williamson et al., 1998; Wang et al., 2001). Magnetic parameters especially χ and S-ratio are affected by dilution caused by precipitation of diamagnetic carbonate and aquatic growth of organic matter. Additionally, under anoxic condition, ferrimagnetic magnetite and titanomagnetite are susceptible to chemical dissolution (Robinson, 1986; Lean and McCave, 1998; Williamson et al., 1998) leading to mineralogical modification of detrital mineralogy. A similar case is seen in Garbayang.

Low susceptibility and S-ratio correspond to two distinct lithological units. The lowest value is associated with eutrophic/ organic rich upper part of Unit-2 and at the base of organic poor varve dominated Unit-1. The consistent higher values are associated with varve/rhythmites successions comprising occasional organic rich laminations.

Geochemistry

A total of 75 samples in the upper part of Units-2 and 3 of the profile were analyzed for major oxides (SiO_2, Al_2O_3, K_2O, Na_2O, CaO, MgO, FeO, TiO_2, P_2O_5) and trace elements (Ba, V, Cr). A few samples were additionally analyzed using bulk powder X-ray diffractometry in order to determine the mineral composition.

Quartz, calcite, illite, chlorite, kaolinite and feldspars (orthoclase, plagioclase) dominated mineralogical composition of the sediments. Abundance of Al_2O_3, FeO and TiO_2 best serves as a proxy of fluctuating meltwater discharge in proglacial lake due to the fact that, these elements are most stable elements in aqueous regime and are produced by physical weathering in glacial terrain (Lisitzin, 1996, Benson et al., 1998)

Chronology

Age estimate at various depths was obtained using liquidscintillation radiocarbon assays and Infra-red Stimulated Luminescence (IRSL) dating techniques. For radiocarbon assays bulk organic fraction of the lake mud was used where as IRSL dating was carried out on sediment blocks.

Radiocarbon dating

Radiocarbon ages obtained on the bulk organic carbon show stratigraphic inconsistency and are shown in figure 4.7. This inconsistency in bulk organic carbon ages can be ascribed to the fact that Garbayang was located in calcsilicate and fossiliferous limestone zone Deevey et al. (1954) first discovered that the organic sediments from alkaline lakes suffer from the hard water effect. Because of this the $^{14}C/^{12}C$ ratios of lake organic carbon are often less compared to time contemporaneous terrestrial counter part. Hence ^{14}C ages of fresh lacustrine deposits could be several hundreds of years old

(Krishnaswami and Lal, 1978). Studies have shown that contribution from limestone carbonate into lake water can result in ^{14}C deficiency (w.r.t. modern atmospheric CO_2) by upto about 25% (Stuiver, 1975). Therefore, the radiocarbon age on organic fraction of such lake sediments tends to be older than their stratigraphic age (Child and Werner, 1999).

Alkaline lakes such as Grabayang have two principal sources of organic carbon viz. the terrestrial plants that utilize atmospheric CO_2 and the aquatic plants which takes varying proportion of atmospheric CO_2 and the dissolved inorganic carbon (DIC). The former draws CO_2 from atmosphere hence require no reservoir correction, whereas the later has to be corrected for reservoir effect. Such variability implies that a simple modern reservoir correction could lead to erroneous age estimates. That is because the hard water conditions likely to change through time and hence the magnitude of reservoir effect is time dependent (Geyh et al., 1998). In view of this the radiocarbon ages on lake sediments located in limestone terrain are to be substantiated by other independent dating method.

Stratigraphic inconsistency of the 8 conventional radiocarbon ages clearly indicates temporal changes in the hardwater effect (Fig. 4.7). In the absence of macrofossils and terrestrial plant material, which are free from reservoir effect (Geyh et al., 1998), the present radiocarbon ages based on the organic mud has limited significance both in terms of climatic inferences and understanding the fluctuations in hard water effect. Difficulties with radiocarbon ages prompted to attempt the optical dating method-using Infra-red Stimulated Luminescence (IRSL) technique.

Infra-red Luminescence dating

In the present study 4-11μm size fraction from predominantly clay rich varve/rhythmites were extracted. A conservative estimate based on Stoke's settling velocity for 4-11 μm size fraction in 30 m water column would indicate that the fine silt fraction will remain in suspension for a minimum of ≥ 50h before sedimentation. Berger (1985) has made similar estimate (≅ 60h) for the fine clay. Thus, the day light exposure of sediment during the transport and sedimentation implies that the fine silt fraction would have seen enough day light for a near complete removal of geological luminescence prior to burial.

Analyses of two samples (GB-1 and GB-6) by Gamma ray spectrometry using hyper pure Germanium detector indicated that decay chains of U and Th were in radioactive equilibrium. Two samples were checked for anomalous fading through a measurement sequence of optical bleaching, beta irradiation and storage in dark for 3 months. The luminescence yield of irradiated + stored sample was compared with an identically irradiated sample measured soon after irradiation. The ratio of the two gives the fading ratio which in the present case was ~1 indicating that the present samples did not suffer from any anomalous fading. Additionally quartz extract of sample GB-6 was dated using the single aliquot regeneration technique of Murray and Wintle (2000).

In the field, sample for optical dating were collected from the lower, organic poor Unit-1 and 2, hence the optical ages are limited to the lower half of the sequence. Figure 4.7 gives the details of stratigraphy along with IRSL and radiocarbon ages. Details of the U, Th and K concentration along with palaeo dose (De), dose rate the IRSL ages are given in Table 4.1. Except for sample GB-7b, IRSL and corresponding radiocarbon ages do not show any correspondence (Fig. 4.7) In fact, where both ages are available the radiocarbon ages are overestimated by > 50%.

Table-4.1

Garbayang

Sample No.	Height (m)	U (ppm)	Th (ppm)	K (%)	Dose rate[+] (Gy/ka)	De (Gy)	Age (ka)
GB-7a	17.85	3.4±0.1	11.1±0 2	3.4±0.2	4.8±0.7	63±7	13±1
GB-7b	7.0	3.4±0.1	11.3±0.2	3 2±0.2	4.8±.07	67±3	14±2
GB-5	4.5	4.1±0.1	13.6±0.1	3.8±0 2	5.7±0.8	95±4	17±2
GB- 6(Q)	2.5	3.6±0.1	11.9±0.3	2.0±0 1	3.0±0.4	51±2	16.7±2
GB-6	2.5	3.6±0.1	11.9±0.3	2.0±0.1	3.8±0.4	63±6	16.6±2
GB-3	1.5	3.7±0.1	12.1±0.2	3.9±0.2	5.2±0.7	93±6	18±3
GB-1	0 5	3.3±0.1	10.9±0.4	4 0±0.2	5.1±0 7	102±10	20±3

Water content taken 20±10%
Cosmic ray dose 150μ Gy/year

Table 4.1 Details of experimental data and IRSL ages obtained on Garbayang lake deposits.

Radiocarbon ages ranged from 14 ka to 34 ka (uncalibrated) but were stratigraphically inconsistent (Fig. 4.7). Compared to this, stratigraphically consistent IRSL ages ranged from 20±3 ka – 13±2 ka and allows us to draw the following inferences.

(i) Around 20±3 ka, the upper lacustrine sedimentation was dominated by varves. Magnetic mineralogy indicate low detrital input around 18±3 ka. Following this a marginal increase in detrital input is seen between 18±3 ka to 13±2 ka, however, it had low magnitude high frequency fluctuations (Fig. 4.8).

(ii) A 1.7 m thick sand horizon was deposited during 17±2 ka which indicate a temporary surge in sediment flux caused by enhanced meltwater discharge (without any discernable hiatus in lacustrine sedimentation).

(iii) The samples do not exhibit anomalous fading (fading ratio ~1). Further a concordance between single aliquot quartz age for sample GB-6 (16.7±2 ka) and the fine grain feldspar age (16.6±2 ka) (Table-4.1) also indicate that the samples

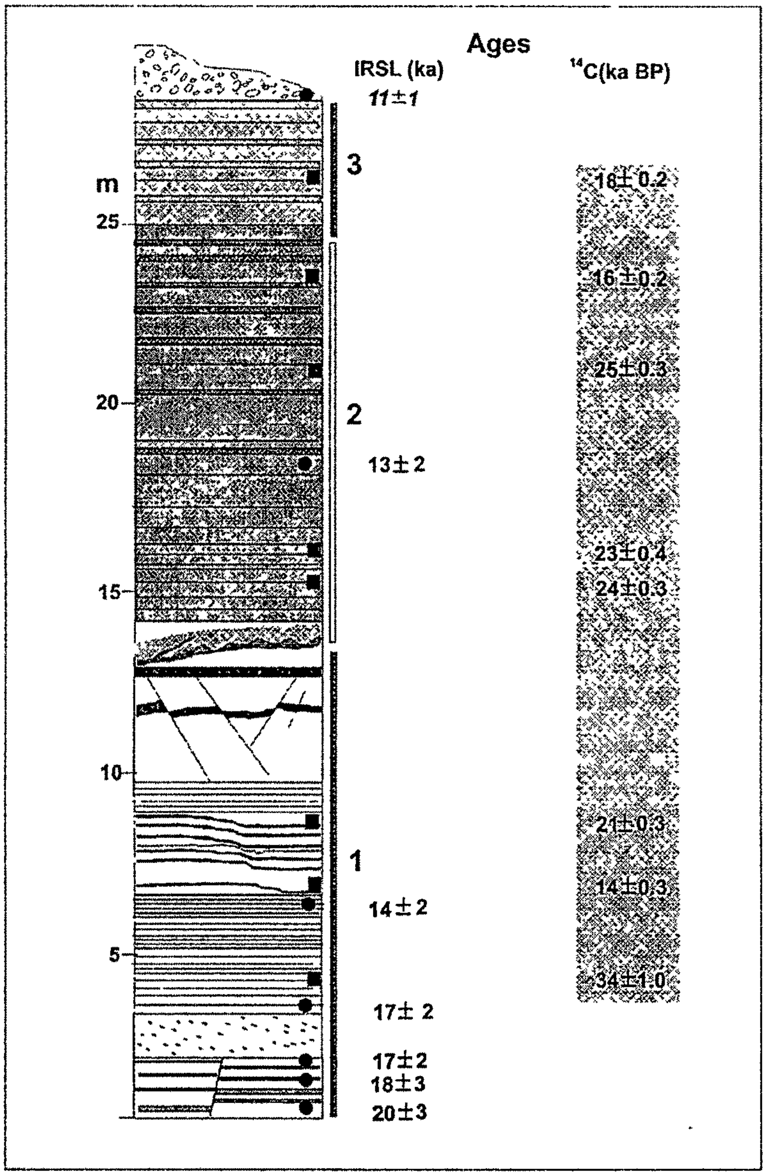

Figure-4.7. Stratigraphy of the upper lacustrine succession, along with IRSL ages (black circle) and stratigraphically inconsistent radiocarbon ages (black cube) obtained on the bulk organic carbon.

were both well bleached and that K-feldspar was free from anomalous fading and/or age underestimation effect.

Palaeoenvironmental Inferences

Unit-1. Sedimentation took place in proglacial calm water environment with highly seasonal water discharge facilitating deposition of distinct laminations representing summer and winter layers (varves). This is also indicated by the occurrence of dropstones that are typical of ice-marginal, glacio-lacustrine environment (Thomas and Connell, 1985).

Unit-2 Presence of intercalating varve and thick organic rich layers (~7 cm), later became more pronounced towards the upper part suggest prevalence of anoxic environment facilitating the preservation of lake organic carbon (Meyers and Ishiwatari, 1995). This unit is overlain by silty-clay rich brownish laminations that are often fragmented.

Unit-3. Dominance of white streaks of calcium carbonate, relative increase in grain size and fragmentary nature of the planar laminations suggests enhance meltwater discharge with low productivity due to frequent fluctuation in lake level. Further occurrences of powdery carbonate streaks (precipitated carbonate) indicate significant change in lake geochemistry. Carbonate precipitation depends on the pH, alkalinity, total dissolved CO_2, and is strongly temperature dependent as the solubility of calcite inversely correlate with temperature (Kelts and Hsu, 1978). These evidences indicate that overall warm water condition prevailed during the deposition of Unit-3.

Unit-3 is overlain by 3 m assorted, rounded to sub-rounded clast supported gravel. Lithology of the gravel comprises calcsilicate and quartzite with sub-ordinate shale, fossiliferous limestone and phyllites. Maximum clast size measured in 1 m x 1 m grids is ~30 cm. The texture of the gravel suggests that deposition was episodic and indicates an abrupt increase in meltwater discharge.

Based on above it can be inferred that the upper lacustrine sequence at Garbayang represents three successive climatic events beginning from clam-oxygenated condition changing into cold anoxic and finally succeeded by warm lacustrine condition.

A low in magnetic susceptibility is seen between 0-2 m at the bottom and is

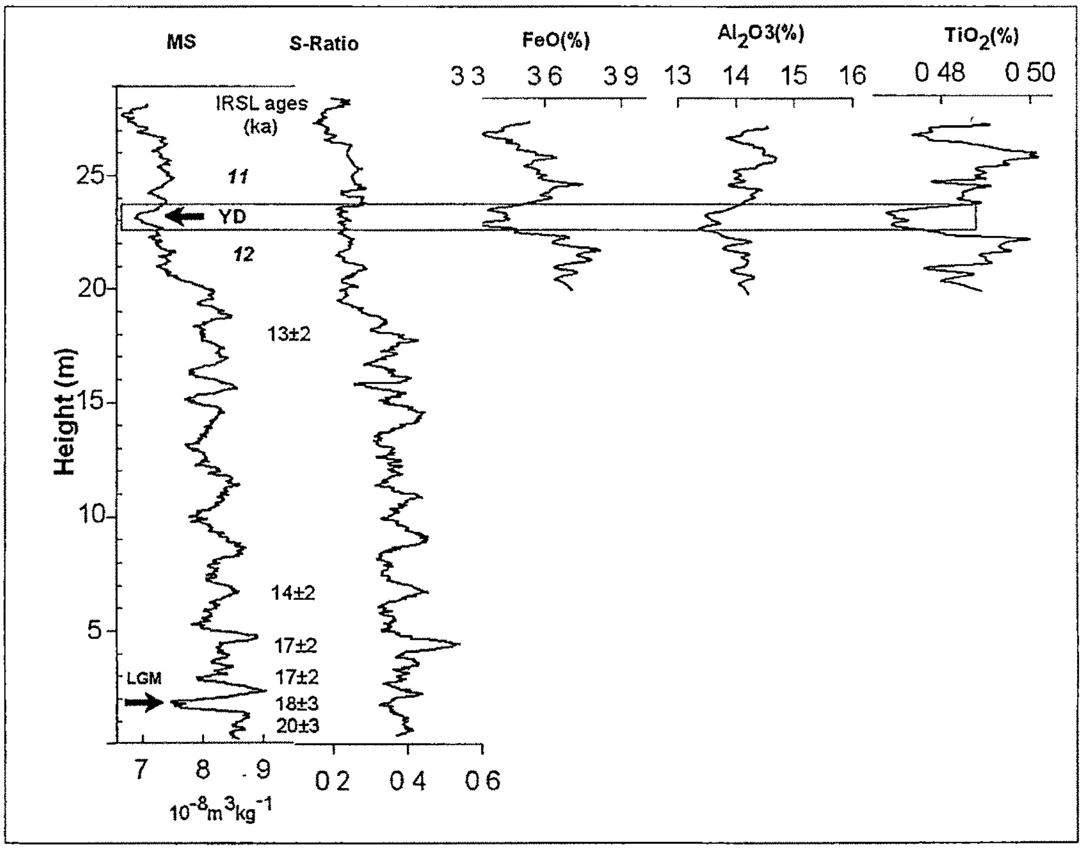

Figure-4.8. Magnetic susceptibility, S-ratio and elemental data plotted against depth. IRSL ages are shown along with the susceptibility curve. IRSL age of *12* ka (22 m height) and *11* ka (25 m height) are interpolated based on the outwash gravel age as discussed in the text. (raw data is given in Appendix-1 and 2).

dominated by varves with low organic matter. Thereafter, though the intermittent varve sedimentation continued but the susceptibility and S-ratio show an increase with low amplitude high frequency changes up to 19 m (Unit-1 and lower part of Unit-2). Towards the upper part of Unit-2, both laminae thickness and organic carbon concentration increases. An abrupt drop in susceptibility and S-ratio corresponding to this unit (between

20 m to 23.5 m) is followed by a rising trend towards the top (Unit-3) (Fig. 4.8). This rise is of a lesser amplitude as compared to Unit-1 and 2 (between 2 m to 20 m).

Sediment input to the lake was exclusively from the valley glaciers located in the basin. The Appi and Nampa valleys were the major contributors. Elemental data from the upper 8 m of the sequence (21 to 29 m) shows average concentration of aluminium (14%), titanium (0.5%), Si (41.4%) and Al/Ti ratio 28.8 which suggest that sediment production by physical weathering with a negligible secondary enrichment through chemical alteration (Lisitzin, 1996). Further, a significant variability in the elemental concentration suggests that the detrital flux into the lake varied through time (Fig. 4.8). Similarly, higher magnetic susceptibility and S-ratio associated with low organic matter suggest an increase in magnetic mineral input due to enhanced erosion in the catchment.

Based on sedimentology, mineral magnetic and elemental data, three environmental end-members can be discerned. To begin with the climate was cold, this was followed by warmer phase with low magnitude high frequency oscillations. The climate again reverts back to cold condition and is succeeded by warming trend towards the top. Subdued discharge during cold dry conditions, led to the deposition of finally laminated varves Though the varve sedimentation continued in warm condition, increased sediment supply and productivity resulted in a shift from varve to rhythmites (upper part of Unit-1 and lower part of Unit-2). Increased sedimentation facilitated rapid burial of organic matter hence its preservation (Meyers and Ishiwatari, 1995). This process also deposited high concentration of detrital titanomagnetite and restricted the dilution of ferrimagnetic minerals by organic carbon. Low amplitude high frequency fluctuation in magnetic data of Unit-1 and the lower part of Unit-2 suggests rapid and frequent fluctuations in terrigenous input and lake productivity during the deposition (climatically governed). Towards the upper part of Unit-2 increasing organic rich laminations at time gave pungent H_2S smell indicating an anoxic environment. Under anoxic condition, ferric iron is unstable and magnetite in particular is susceptible to dissolution (Lean and McCave, 1998). Low Al, Fe and Ti, low susceptibility and low S-ratio between 20 m to 23.5 m indicate eutrophic condition due to reduced meltwater discharge suggesting a cooler event (Fig. 4.8). IRSL age of the outwash gravel at Goting (11±1 ka) with identical geomorphological setting and stratigraphy to that of Garbayang, this event is bracketed between 13±2 ka - 11±1 ka.

Since the sediment characteristics between 17.85 m and 28.4 m are broadly identical, a linear sedimentation rate could be reasonably assumed in order to estimate the timing and duration of this cooling event. In doing so extreme minimum age of 10 ka for outwash gravel has been considered (age minus error). Thus an interpolated age of 12 ka is obtained for height 21.35 m and 11 ka age for height 24.85 m (Fig. 4.8), which coincides with the timing of Younger Dryas- a major postglacial cooling after Heinrich event-1 (Bond et al., 1993; Adams et al., 1999; Alley, 2000). Dated between 12,900 – 11,500 years ago (Adams et al., 1999), the Younger Dryas event resulted in the weakening of NE trending Gulf stream in Atlantic ocean with consequent cooling (Adams et al., 1999). Chronological evidence of postglacial cooling related to Younger Dryas from Indian sub-continent are scanty except for reports of changes in the hydrological regime in Thar desert (Kar et at., 2001). In view of this, the present evidence is significant suggesting inter hemispheric nature and near synchronicity of the cooling event

Goting

The varve deposits at Goting in the Higher Central Himalaya, first reported by Sastri et al., (1970) and assigned an interglacial stage, were reinvestigated by Pant et al. (1998) to delineate geological and morpho-structural setting of the Goting basin and reconstruct the palaeoenvironment. They concluded that varves were deposited in a proglacial-lake that came into existence on the retreat of main Dhauliganga valley glacier. Using radiocarbon dating method on lake organic carbon, it has been suggested that the deposition commenced around 40 ka and probably continued till the glacial maximum (~20 ka). However, with the discovery of hard water effect in samples from Garbayang lake sequence, a renewed effort towards obtaining alternate chronology for Goting samples was undertaken using luminescence dating technique.

Geology and Geomorphology

The Khal Kurans ridge marks the southern limit of the Goting basin that is the subtle surface expression of the Trans Himadri Fault (THF) and separates the Central Crystalline rocks from those of Tethyan Group (Fig. 4.9). Undifferentiated Precambrian gneisses and schists are exposed to the south of the THF and towards the north these are juxtaposed against a succession of Martoli Group of rocks including rocks of Ralam and Garbayang Formations of Cambrian age (Sinha, 1989). Khal Kurans ridge rises abruptly above the surroundings and forms the southern limit of the Goting basin. Further towards northwest, THF has generated series of fault scarps and has created numerous rockfall debris in the basin. This rock debris at times seen mixed with the Quaternary clays and has been mistaken for moraines by the earlier workers (Sastri et al., 1970). The Dhauli Ganga flows in N-S direction and bisects the Goting basin into two halves. The flow is braid meandering type in the basin, which becomes torrential once the river crosses Khal Kurans ridge (Fig. 4.10A). At Khal Kurans it takes a sharp NW-SE turn following the

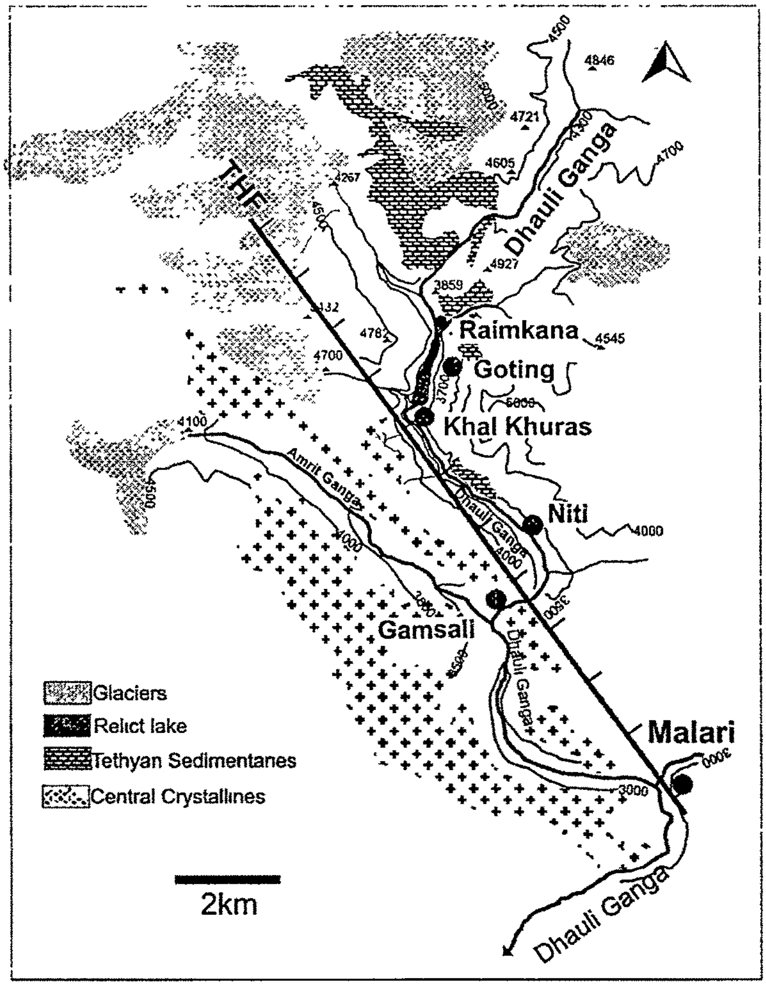

Figure-4.9. Map showing major lithology and geomorphic features between Malari and Goting. At Khal Khuras Dhauliganga flows parallel to the THF and cut across at Ghamsali and Malari. At Malari a spectacular gorge has been carved (after Sinha, 1989; Valdiya, 2001).

THF and has cut ~500 m deep gorge (Fig. 4.10B). The valley floor has a gentle gradient and has an average elevation of 3820 m. Khal Kurans ridge acted as geomorphological barrier and has played an important role in preventing the advancement of Quaternary glaciation. There are ample evidences to suggest that the terminal moraine of the

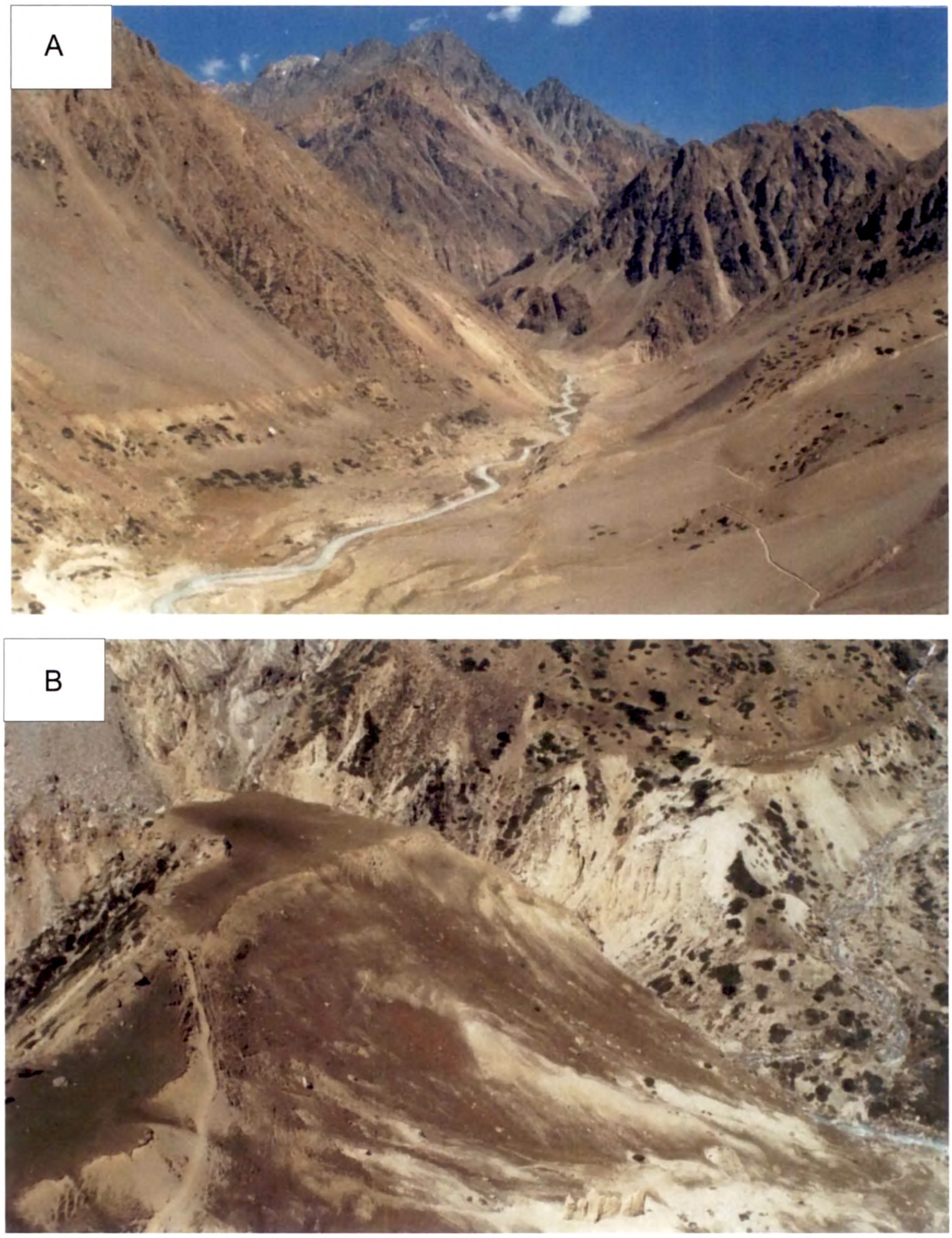

Fig 4.10 A Goting basin, sky line is Indo-Tibetan water divide. Incised outwash gravel seen left, Dhauli Ganga flows as braid meandering river.

B Goting basin towards south west, Khal Kurans ridge seen as table land. Relict lake deposits appear as pinnacles in the fore ground. Dhauli Ganga flows through a deep gorge after incising the outwash gravel, lake deposits and the terminal moraines in descending order seen towards the right.

advancing valley glacier blocked the narrow opening at Khal Kurans. Following its retreat, a proglacial lake was formed in which near continuous sequence of rhythmites and varves were deposited.

Physical stratigraphy and sedimentology

The basin floor is covered with ground moraines. Lateral moraines are absent or are concealed under the talus debris and the clay draps of relict lake deposits. However, lateral moraines are traceable upstream at the confluence of Dahuli Ganga with Raimkana which forms the northern end of the palaeo-lake (Fig. 4.9) as was evidenced by the occurrence of the lake deposits overlying them. The moraines are overlain by rhythmites and varve succession, which are in turn succeeded by a 8 – 10 m thick outwash gravel that constitutes the top most lithofacies in the basin. The ground moraine appears at the base of the lacustrine deposits show distinct subglacial features of a lodgment till incorporating huge boulders with smoothened convex tops. At places the lodged diamicts also show shear surfaces. In general the moraines are deformed and contain undifferentiated diamicts. These have therefore, been described as ground moraines. However, the lodged and other forms of diamicts definitely suggest that the glaciers must have extended up to Khal Kurans ridge that formed a natural barrier. In addition, there are huge deposits of push or end moraines seen on either side of the Dhaulganga gorge covering the base of the Khal Kurans ridge and riding over it (Fig. 4.10B). It is therefore, suggested that the narrow opening of the Dhauli Ganga was blocked by the end moraines aided by the natural rampart formed by the Khal Kurans ridge (Fig. 4.10B), a situation similar to the Garbayang basin. The lacustrine condition prevailed after the partial recession of the valley glacier to the conflence of Dhauli Ganga and Raimkana towards the north that also limits the northern extension of the proglacial lake in Goting basin. Presently Dhauli Ganga has deeply incised the lake deposits and has exposed the sequence that has been found preserved towards the sheltered left flank (Fig. 4.10B).

In the incised section exposed towards the left flank of Goting basin the lower part (~10 m) is concealed under the slump where as the upper 15 m is truncated. Towards the top ~10 m thick outwash gravel marks the termination of lacustrine sedimentation (Fig. 4.10B). In the present study only the exposed 12 m thick varve succession could be sampled. The section can be divided into two major units. The lower Unit-I between depths 40 to 34 m (in composite stratigraphy) shows presence of thicker laminations (~2-5 cm) and dominated by fine silty clay with frequent occurrence of ice rafted debris (Fig. 4.11). At places thick organic rich laminations are also encountered. Sequence in this part is more like rhythmite in character suggesting relatively high meltwater discharge. Besides this, horizon also shows evidences of palaeoseismic activity in the form of seismites (Fig. 4.11).

The intercalated ice rafted debris suggests prevalence of ice-marginal, glacio-lacustrine environment (Thomas and Connell, 1985). Such debris that is plucked by ice from the surrounding lithology is gradually released once ice melted out. Melting can be caused both by solar irradiation and subaqueous under melting caused by gradual heat transfer from lake water to ice. This results in the loss of embedded material, fine particles settle slowly, but material of sand size and larger will drop down rapidly forming "Xenoliths" or even a continues sheet of melt out material. They are also called the drop stones in a situation where the occurrence is sporadic (Brodzikowski and VanLoon, 1991). Their presence would imply higher solar insolation/lake water temperature.

This is followed by Unit-II between depths 35 m to 25 m (truncated top), sediments are dominantly varvite in character (Fig. 4.11). They show alternating bundles of internally laminated ash gray, and fine silty limonitic horizons appearing regularly at 5-8 cm intervals. A single varve consists of millimetre to sub-millimetre scale couplet of a dark and light-coloured lamina, composed exclusively of fine silt and clay and devoid of any coarse silt. Usually the laminae have fused together and difficult to discern the annual layers in a hand specimen, however under the microscope they are well differentiated (Fig. 4.4C).

Sediments in most proglacial-lakes are sensitive to climate processes by virtue of their sensitivity towards hydrological changes, hence can be used to reconstruct a high-resolution record of climate change. In view of this, variation in the texture and sedimentary structures of Goting lacustrine deposits may have climatic implications. While the rhythmites along with ice rafted debris may be indicative of enhanced runoff that may indicate mild climatic oscillations during their deposition (Barry, 1992). Similarly the varve sedimentation towards the upper part would suggest reduction in meltwater discharge possibly caused by decrease in the temperature. These observations find support in the magnetic susceptibility (χ) and geochemical data as discussed in the succeeding section.

Magnetic and Geochemical studies

Two hundred sediment samples collected at 3 – 5 cm interval were analyzed for magnetic susceptibility, major oxides (SiO_2, Al_2O_3, K_2O, Na_2O, CaO, MgO, FeO, TiO_2, P_2O_5) and selected trace elements (Ba, V, Cr) using X-ray Fluorescence Spectrometry. Some samples were also analyzed using bulk powder X-ray diffractometry in order to show the presence of magnetite with varying amount of haematite. Magnetic mineralogy determinations like IRM acquisition and thermal demagnetisation of IRM and thermomagnetic runs of χ from room temperature to 700° C further confirm the presence of magnetite in the samples. Fluctuations in χ are in phase with the magnetomineralogic S ratio, simplified here as the ratio of $IRM_{0.3T}/IRM_{2.5T}$ that is a measure of the proportion of magnetite to haematite in the sediment. Higher S values indicate predominance of magnetite relative to haematite. Magnetic susceptibility correlates well with temporal variations in total iron indicative of detrital Fe flux

In case of major oxides analyzed, the abundance of Al_2O_3 and TiO_2 best serves as a sensitive proxy of climate change. Changing proportions of Al_2O_3 compound is believed to reflect changing proportions of clay mineral abundance that in turn, manifests weathering intensities in the provenance (source region). In view of geomorphological setting of the Goting basin, the predominant source of sediment has to be the lateral or end moraines of the retreating valley glacier, located at the proximal end of the ambient lake. Therefore, in addition to the primary clays produced by the glacial grinding, weathering of moraines during warmer intervals could also facilitate alteration of feldspathic minerals (orthoclase, plagioclase) to clays. Hence increased fluxes of Al_2O_3 document the additional clay production to the detrital clays. Similarly, TiO_2, which has low solubility, is the product of glacial grinding (Benson, et al., 1998). It gets incorporated in the lake sediments through the glacial melt waters. Therefore, the relative abundance of this mineral is a good indicator of the sediment fluxes received into the lake during the warmer periods. In case of varves, the effect of mechanical fractionation between clay rich (winter) and carbonate and silica rich layers (summer) during settling is discounted because chemical analyses were run on sediment samples that cover 3-5 cm intervals in the stratigraphic record.

Chronology

As discussed earlier, the lacustrine organic carbon in Goting also indicates varying proportion of dead carbon contamination from the surrounding limestone terrain. This is demonstrated in radiocarbon chronology, shown along with the IRSL ages in figure 4.12.

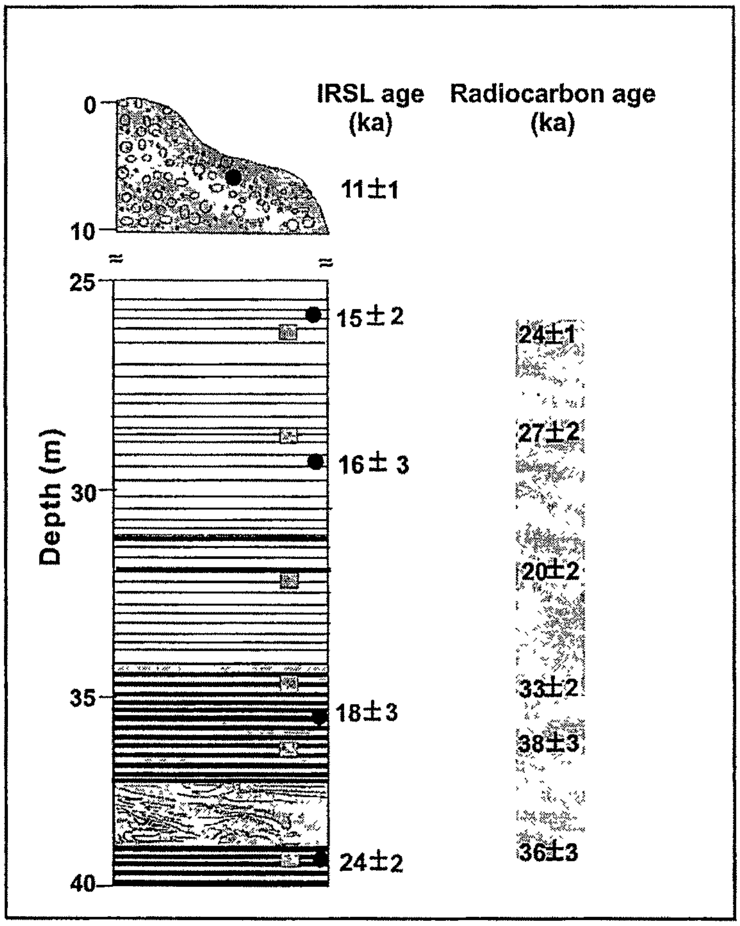

Figure-4.12. Stratigraphy of the lacustrine succession at Goting. IRSL(black circle) and radiocarbon ages (grey cubes) are shown along side the log.

In the subsequent discussion, IRSL chronology has been used.

The IRSL age at depth 39.5 m is 24±2 ka whereas towards the top at depth 26 m yielded an age of 15±2 ka. Two more ages at depth 29 m and 36 m yielded 16±3 ka and 18±3 ka respectively (Fig. 4.12). Single aliquot BGSL age on coarse grained quartz from over lying outwash gravel (depth 5 m) at Goting gave an age of 11±1 ka (GT-1) (Table-4.2). The chronology help in drawing the following inferences

(i) Since the sequence continue below 39.5 m depth, it can be inferred that sedimentation in the proglacial lake would have commenced much before 24±2 ka.

(ii) The truncated upper section suggests that sedimentation would have continued after 15±3 ka and before the deposition of outwash gravel dated to 11±1 ka.

(iii) Deposition of the outwash gravel marks the termination of lacustrine environment around 11±1 ka.

Goting

Sample No.	Height (m)	U (ppm)	Th (ppm)	K (%)	Dose rate (Gy/ka)	De (Gy)	Age (ka)
GT-1	5	4.1±0.1	13±0.2	3.2±0.2	4.7±0.3	55±3	11±1
GS-8	26	7.3±0.1	24±0.3	4.1±0.2	7.8±1.0	119±6	15±2
GS-7N	29	7.4±0.1	24±0.3	4.8±0.2	8.2±1.0	135±15	16±3
GS-5N	36	6.7±0.1	22±0.3	5.2±0.3	8.1±1.0	151±9	18±3
GS-1	39.5	8.3±0.1	21±0.4	4.6±0.2	8.2±1.0	182±10	24±2

Water content taken 20±10%
Cosmic ray dose 150μ Gy/year

Table 4.2 Experimental data and IRSL ages obtained on Goting lake sediments.

Palaeoenvironmental inferences

Sedimentological evidences indicate the prevalence of two distinct climatic regimes. Presence of thicker organic rich silty laminae (rhythmites) and frequent occurrence of ice rafted debris in the lower Unit-I suggest enhanced sediment supply and higher surface water temperature. The overlying varve dominated Unit-II indicate cooler condition. These observations find support in the magnetic susceptibility and geochemical data.

Enhanced magnetic susceptibility and major elemental concentration during the deposition of Unit-I indicates high sediment flux. IRSL age bracket this unit between 24±2 – 18±3 ka (Fig. 4.13). Since sediment flux in a proglacial lake is controlled by the meltwater discharge, it is reasonable to assume that during 24±2 ka to 18±3 ka higher solar insolation led to enhanced glacial melt in the region. Evidence towards enhanced melting is also supported by sedimentological data. Over all climatic deduction based on sedimentological, magnetic susceptibility and elemental data indicate a relatively warm condition with less frequent oscillation prevailed between 24±2 ka to 18±3 ka.

This is succeeded by varve dominated Unit-II. Geochemical and susceptibility data (Fig. 4.13) show a sudden decrease after 18±3 ka (depth 35 m) that continues beyond 16 ka (depth 30 m). However, fluctuations were of smaller magnitude, but had higher frequency compared to Unit-I. This suggests that though the climate was significantly cooler compared to the Unit-I, it was punctuated by frequent warm oscillations.

Hence a phase of climatic instability during the period 18±3 ka to <15±12 ka can

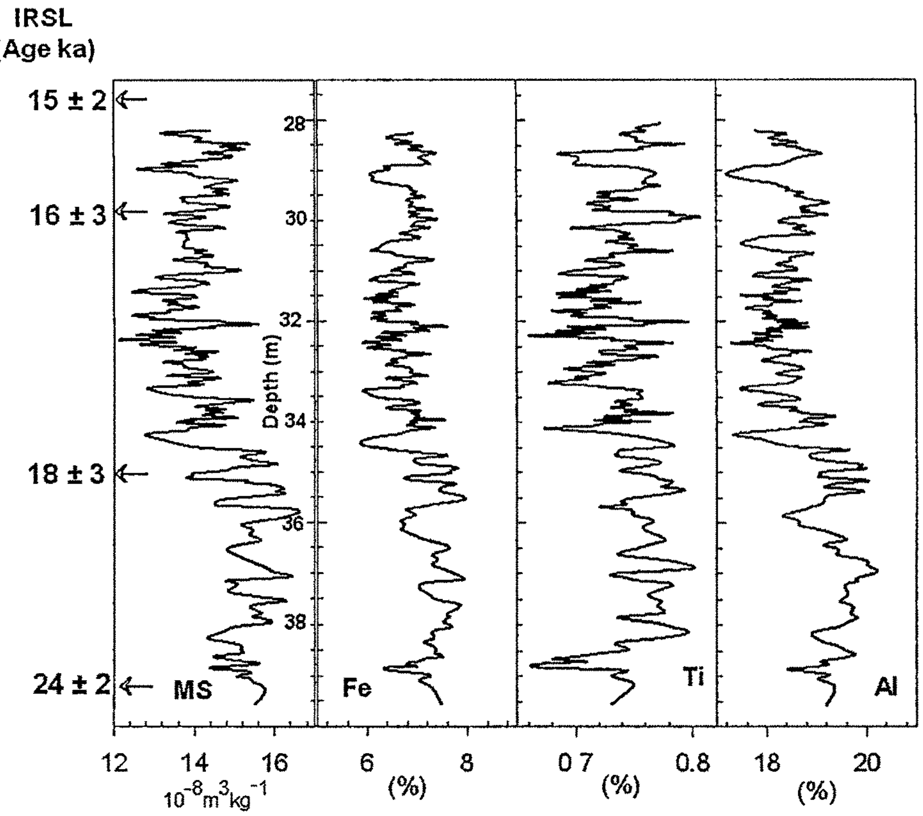

Figure-4.13. Plot of magnetic susceptibility and elemental data along with the IRSL ages. Two climatic domains are clearly seen. A high sucseptibility and elemental concentration below 18 ka and a low susceptibility and elemental concentration above 18 ka. These variations correspond to Unit-I and II respectively (raw data is given in Appendix-3).

be inferred (Fig. 4.13). Horizon corresponding to the Younger Dryas cold event is not located due to the truncated nature of the upper sequence where deposits younger than 15±2 ka are non-existent. Finally the upper most outwash gravel that has been dated to 11±1 ka indicate commencement of Holocene wet phase in the region.

Evidence of Quaternary seismicity

Two important structural features with very different characteristics developed in the Himalayan orogen are (i) the north dipping thrusts (compressional structures) such as Main Central and Main boundary thrusts and (ii) the east striking, north dipping normal faults – the South Tibetan Detatchment Systems (Coleman and Hodges, 1995). Called as the Trans Himadri Fault (THF) by Valdiya (1987) is an equivalent of the South Tibetan Detachment Systems (STDS) developed near the crest of Higher Himalaya along the southern margin of Tibetan plateau to accommodate topographical and crustal thickness arising from a subducting Indian Lithosphere (Burchfiel and Royden, 1985). In contrast, the southern Tibetan plateau developed by an east-west extension and north striking and east and west dipping normal faults and associated strike slip structures (Molnar and Tapponier, 1978; Ni and York, 1978). It has been suggested that in the tectonic evolution of Himalaya and Tibet, THF played an important role by providing accommodation space to the strain gradient arising out of east-west extension in southern Tibet and north-south compression in the Himalaya (Hurtado Jr. et al., 2001).

In Central Himalaya THF is located in the upper reaches of the Dhauli Ganga, Gori Ganga and Kali river basins and separates the low grade Tethyan metasediments from the Greater Himalayan gneisses (Valdiya, 1987; 2001) (Fig. 4.2). Additionally, at places the north striking, east-west extensional features of Southern Tibet are located in Nepal Himalaya (Arminjo et al, 1986; Edwards and Harrison, 1997; Hodges, 2000), which at places extend close to THF in the Central Himalaya.

There is reasonable agreement that initiation of THF started along with the formation of MCT in Miocene (Hodges et al., 1992; Edwards and Harrison, 1997). Based on dating of intrusive bodies (leucogranite) using U-Th-Pb and $^{40}Ar/^{39}Ar$ (crystallization and cooling ages) it has been suggested that formation of THF took place during 24-19 Ma. (Hodges et al., 1992; Harrison et al., 1995b). More recently, crystallization ages obtained on leucogranite using Th-Pb systematic in Bhutan Himalaya yielded an age of 12.5 Ma. This suggests that a significant orogen-normal extension in southern Tibet continued till 12.5 Ma. This is ~10 Ma later than previously recognized (Edwards and Harrison, 1997) Compared to this the N-S Yadong-Gulu rift system that cuts across 12.5

Figure-4.14. Field photograph showing the geomorphic manifestations of THF in Goting basin such as perched glacial valley, fault scree, incision of outwash gravel and lacustrine deposits.

Ma THF in eastern Nepal (Edward and Harrison, 1997) indicates that the north directed extension must have ceased before the initiation of N-S rift system in the southern Tibet. Thermochronometric results of deeply incised valleys in the vicinity of Yadon-Gullu rift system in Tibet (NW of Lhasa) suggest that initiation of rift started around 8 Ma (Harrison et al., 1995a; Harrison et al., 1998). Though both extensional features (N-S and E-W) indicate gravity driven dissipation of potential energy, however, it started early in the Higher Himalaya compared to that in the southern Tibet.

Numerous geomorphological evidence from the southern Tibetan plateau suggest normal faulting since Pleistocene associated with the east-west extension (Armijo et al., 1986). Compared to this, though the structural and geochronological data indicate that the THF was active during the Miocene (Hodges et al., 1998; Edward and Harrison, 1997; Murphy and Harrison, 1999), its subsequent activation remains poorly understood. Recent evidences from Thakkhola graben in Nepal suggest that movement of THF persisted either episodically or continuously during the Quaternary (Hurtado Jr. et al., 2001). Wu et al. (1998) suggested the possibility of the north trending rift in Nepal Himalaya acting as a transfer fault during the movement on THF. Hurtado Jr. et al., (2001) proposed that east-west extension and north-south extension were related process in recent geological times.

Observations on geomorphological features and relict lake deposits in the vicinity of THF are presented here. Geomorphological features include (i) truncated scree fans (ii) incised fluvial terraces (iii) terminated glacial moraines (iv) perched and abandoned glacial valleys and (v) abrupt steepening of river gradients (Figs. 4.14 and 4.15). Evidence preserved in relict lake deposits are (i) contorted laminations (seismites) and (ii) faulted laminations. Observations along with the luminescence dating indicate that these structures (east-west and north-south) remained active during the Late Quaternary and the activity continued during Holocene.

The study area lies north of Central Crystalline massif in the rain shadow zone of Central Himalaya (30°5-30°49' N and 79°20'- 80°50' E, Fig. 4.2). THF demarcates two contrasting topographies viz (i) the deeply incised "V" shaped valleys and snow clad Trans Himalayan ranges towards the south and (ii) a gentler rolling topography with broad "U" shapes valleys towards the north. From NW to SE, three major rivers viz. Dhauli Ganga, Gori Ganga and the Kali Ganga, originate from the valley glaciers and drain the area.

Glaciogenic features such as broad 'U" shape valleys are at times associated with

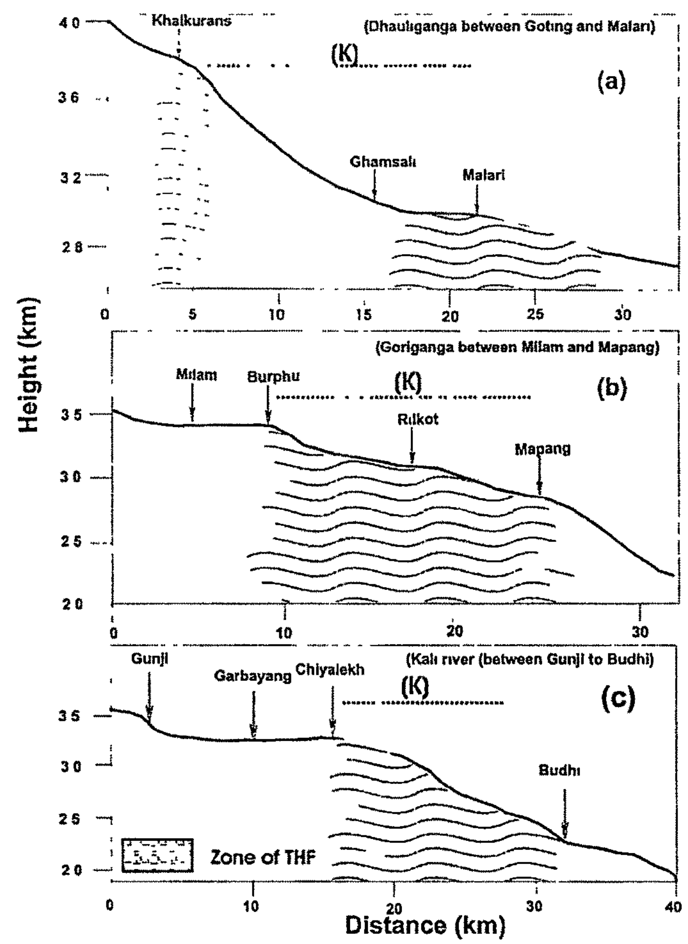

Figure-4.15. Longitudinal river profiles in the vicinity of THF show over steepening of river courses. Such changes in river profile are spread over a distance; hence we call them knick zone (K). In Goting basin two such zones have been identified that is because Dhauli Ganga after emerging from Khal Kurans, flows parallel to the splays of THF and cut it across at Ghamsali and Malari. At these locations the river has carved deep gorges. Suspected zone of THF is shown with wavy notation.

tillites, relict proglacial lake deposits and outwash gravel terraces are some of the major geomorphological features in the area. The river basins can be broadly grouped under two flow regimes, a sluggish, meandering fluvial course with occasional braid bars towards the north of the THF (Fig. 4.10A) and the fast cascading torrential types immediately to its south. These two contrasting regimes are differentiated by distinct breaks in slope (knick zone) across the THF and are invariably associated with deep gorges (Fig. 4.15).

North-South extension

Geomorphological Evidence

Surface manifestation of the THF is expressed as NW-SE trending discontinuous linear ridges comprising crystalline rocks that rise abruptly towards the southern flank and constitute the footwall of THF. Geomorphological evidences can be grouped under two categories of landforms, (i) those associated with north-south extension (THF) and (ii) those related to east-west extension (north striking basins). Rivers emerging from the THF show sudden steepening of their course-giving rise to knick zones (eg. Khal Kurans, Malari, Rilkot-Mapang and Chhiyalekh; Fig. 4.15A, B and C). Such deviation in river course is associated with resistant crystalline rocks located towards the footwall of the THF, whereas gentle river profiles are associated with the hanging wall of less resistant Tethyan sedimentary rocks. This is in accordance with the observation that upstream of an axis of uplift, the channel gradient and valley floor slope is reduced, where as below the axis they are increased (Burnett and Schumm, 1983).

Furthermore, lithologically controlled knick points usually develop on less resistant rocks and migrate upstream with time. Contrastingly, knick points associated with active tectonic structures are stationary due to continued activity in a specific zone. In the present case since knick points are confined to a narrow zone of THF and associated with resistant crystalline rocks, it implies that they are not formed due to a differential resistance of lithology to erosion. Seeber and Gorntiz, (1983) reported similar evidences of pronounced steepening of river course that are associated with the MCT and more resistant crystalline rocks and less steepening with the MBT (less resistant metasedimentary rocks) and attributed this to on going tectonism along MCT.

Perched glacial features such as the raised "U" shape valleys, abrupt termination of lateral and end moraines e.g. at Goting basin near Khal Kurans ridge (3200m), Shalang basin at Rilkot (3100m) and in Garbayang basin at Chhiyalekh (3100m) are the other morphological manifestations of on going seismicity along THF (Figures 4.14 and 4.16). In all these cases the footwall of THF acted as morphological barrier against the advancing valley glaciers in the region.

Sedimentological Evidences

Garbayang and Goting basins that are ~200 km apart provide identical morphotectonic and hydrological setting along with similarity in the upper lacustrine record (Fig. 4.2, 4.3 and 4.11). In these basins, laminated sediments were deposited under subaqueous conditions. Such sediment records liquefactions and other deformation structures (seismites) are produced by the passage of shock waves associated with seismic events (Ringrose, 1989; Seilacher, 1969; Sims, 1975). Varve laminations in these sediments suggest deep-water condition with water stratification (Rodriguezpascua et al., 2001). Such laminations are conducive for the development and distribution of shear planes preferably at sediment water interface (Maltman, 1987). Varve and rhythmite successions at Goting and Grabayang basins have preserved evidence of palaeoseismicity in the form of seismites and vertical displacement of planar beds.

Evidence of palaeoseismicity at Goting is limited to the lower part of the section and

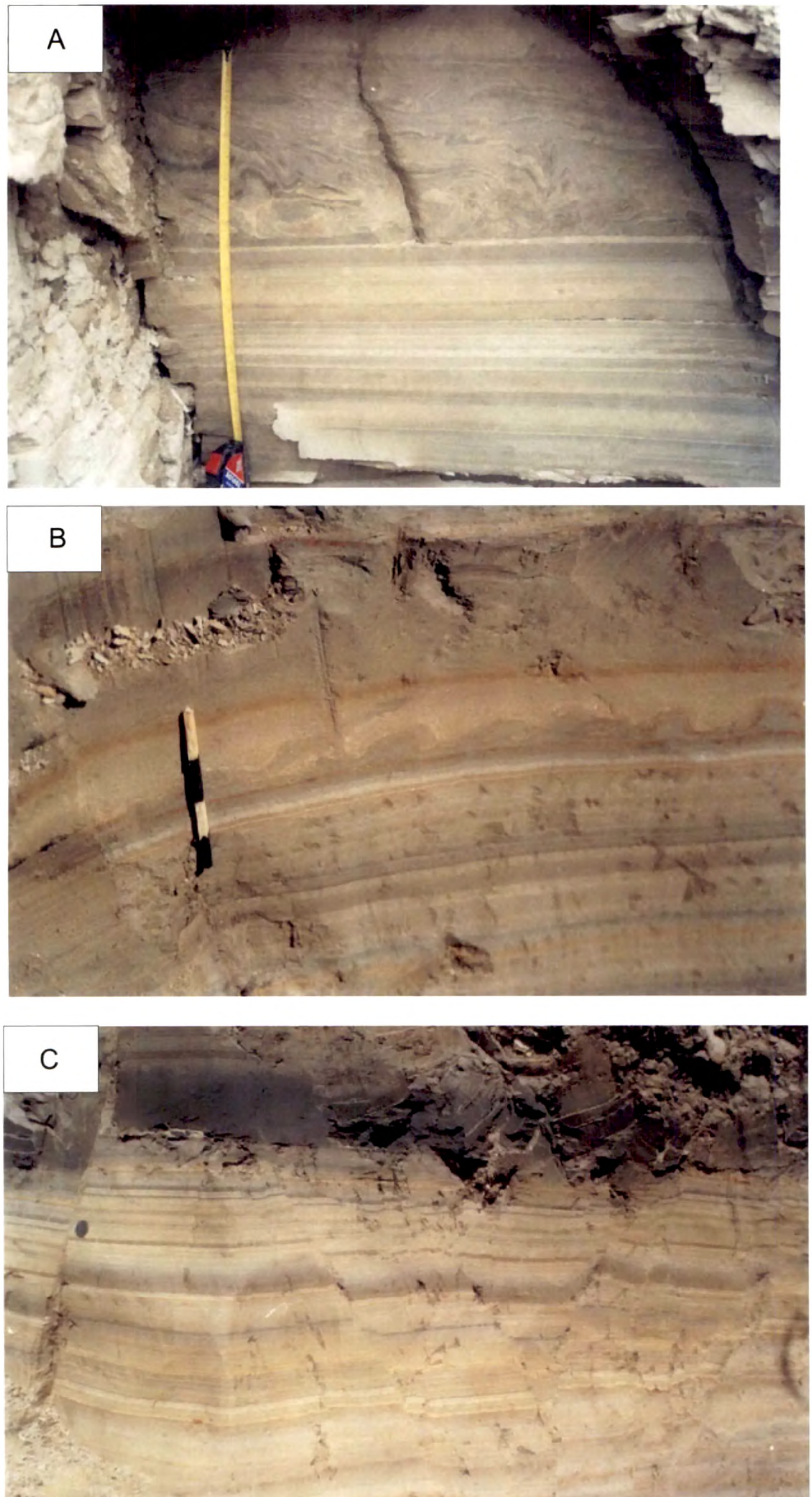

Fig 4.16 A Seismites at Goting.
B Flame structure (mixed layer) at Garbayang.
C Horst and graben structure at Garbayang.

sandwiched by undeformed planner laminations (Figs. 4.16A and 4.17; Goting). The deformed laminations comprise mm to cm scale asymmetrical folding, small scale faulting caused by localized silt intrusion (water escape structure) into overlying organic rich clay lamina, convolute lamination (pressed as narrow anticlines). The upper part of the deformed horizon shows flowage structure (pseudo thrusting) (Figs. 4.16A and 4.17).

The upper 30 m section that was examined at Garbayang show four distinct events of seismicity termed as event-I to event-IV in ascending order (Fig. 4.17; Garbayang). Event-I and III are the brittle deformations, event-II is a ductile shearing and event-IV show flame structure that is similar to the mixed layer of Marco and Agnon, (1995). Flame structure is associated with varve-like laminite in which sub-horizons could be differentiated from bottom to top: (i) basal undisturbed lamina (ii) folded lamina and (iii) fractured and fragmented lamina (Fig. 4.16B). The top of the mixed layer is overlain by undisturbed planar laminae. Such features have been attributed to a seismic shaking at sediment water interface of magnitude >5 (Marco and Agnon, 1995). Similarly undisturbed planer beds separate the faulted laminae. The displacement in faulted laminae increased progressively along the fault plane from event-I to event-III. In addition, a wide variety of faulting geometries with predominance of brittle shearing was seen. Ductile shearing was seen only in event-II. The fault surfaces for all events are either north or south dipping. In event-III the fault surfaces dip towards northeast and southwest with high dip amounts (>60^{0}) that has given rise to mini horst and graben structures (Fig. 4.16C and Fig. 4.17; event III.). The dip amount however varies significantly along the fault trace in some cases. The displacement surfaces are planar to slightly sinuous. The length of fault surfaces as seen in cross section varies from less than few mm to as large as two meters.

The faulted sediments are dominantly planar, dip at high angles and strike perpendicular to underlying hard rock at around ~150 m depth. Thus, faults are unlikely to

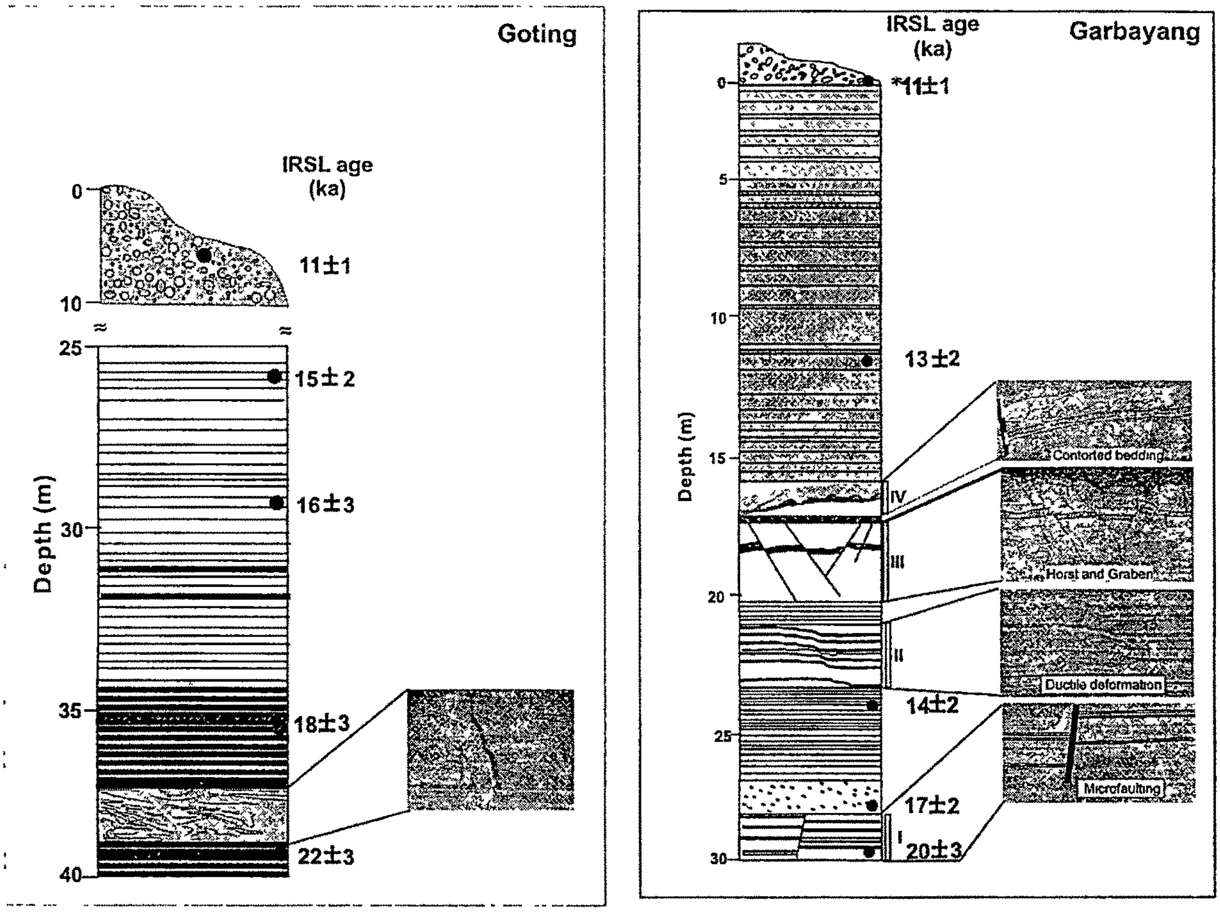

Figure-4.17. IRSL chronology of seismically induced deformations in the lacustrine succession at Goting and Garbayang. IRSL age of 11± ka at Garbayang is extrapolated from Goting.

be related to a small-scale detachment along the contact between the varves and hard rock. Additionally, gravity slide would not have caused the faulting. Had that been a case, the fault strike would have been parallel to the strike of the basin (NE-SW). Instead the fault strikes perpendicular.

Conventionally it has been suggested that conjugate faults reflect a widespread extension feature. In general, conjugate structures form either through the intersection of oppositely directed faults that have a common origin or through a chance intersection of two individual faults that nucleate at separate points in space (Nicol et al., 1995). Absence of congruence between slip profiles along oppositely directed fault planes in the conjugate set of fault event-III suggest a chance intersection of two independently nucleated faults. This indicates that the faulting events most probably are amalgamation of episodes of rapid recurrent seismicity rather than isolated single event

Finally, though at times it is difficult to uniquely establish coseismic origin of the individual features as discussed above, however, their abundance, the close association of different deformational style and proximity to the major structure suggest that they are seismogenic (Meghraoui et al., 2000). Further confidence in this inference accrues from the fact that Goting and Garbayang basins have comparable morphotectonic and hydrological setting and have a near identical palaeoseismic evidence.

East-West extension

Observations using satellite remote sensing data (IRS 1D LISS-III, October 1997) show the presence of two linear depressions that originate in southern Tibet, cuts across the Himalayan arc and extends close to the THF in Goting and the adjoining Alaknanda basin (Fig. 4.18). These depressions suggest their formation related to east-west stretching analogous to the formation of extensional features like the Thakkhola graben and the Yadong-Gulu rift in Nepal and southern Tibet (Hodges, 2000). Due to paucity of cloud and snow free satellite data, other basins could not be explored. However, topographic maps clearly show a linear depression extending into southern Tibet in Shalang basin. It is suggested that in all the three basins viz. Goting, Shalang and Garbayang, evidence of Late Quaternary deformations are associated with east-west extension. This is because, in Shalang basin ~1 km lateral shift (due west) in valley glacier is observed (Fig. 4.19). A sequential migration of valley glacier left behind lateral moraines corresponding to glacial advancement stage-I to III. Further, immediately below the snout of the glacier a vertical incision ~80m is seen and the present day Shalang glacier overrides the Nanda Kot ridge. Thus, indicates a differential movement in north striking basin with preferential rise of the western flank (Fig. 4.19).

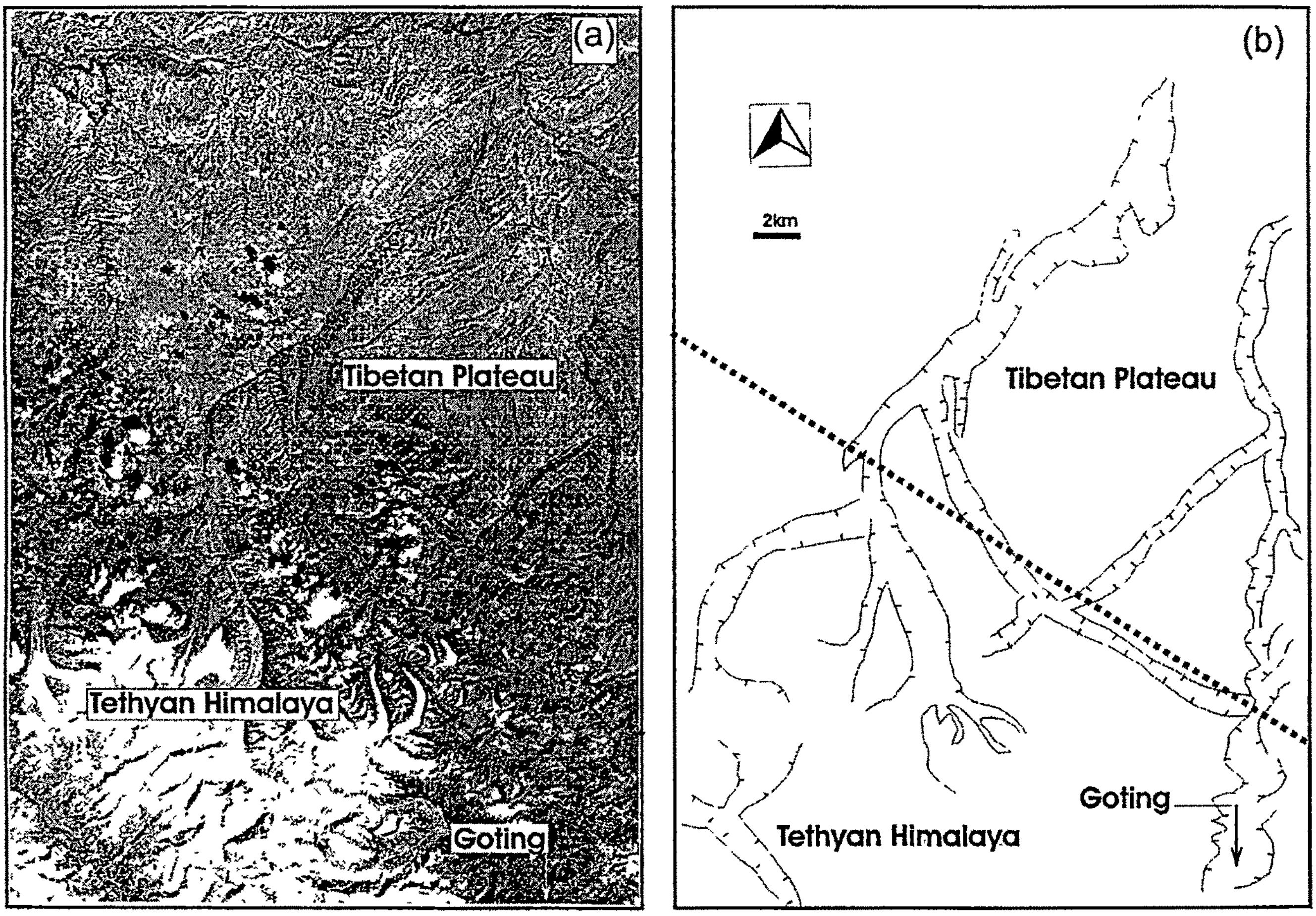

Figure-4.18. False colour composite of IRS 1D, LISS-II, October 1997 data showing area north of THF between Goting and Badrinath basins. (a) Two north-south trending rifts can be seen cutting across the Himalayan arch. (b) Line drawing of the two major rifts identified. Dotted line represent watershed boundary between the Himalaya and southern Tibetan plateau.

An evidence of seismic activity related to east-west extension during Holocene to present is seen in four incised outwash gravel terraces in the Goting basin (Figs. 4.20A and B) that abut the western Semkharak. The eastern flank has preserved only the older T_1 and younger T_4 terraces. Terrace T_1 is unpaired and lies at a lower elevation compared to the western flank suggesting differential movement after their formation. A scree cone emanating from western flank truncates on top of the oldest terrace T_1. Vertical offset between terrace decreases from T_1 (20 m) to T_4 (5 m). Outwash gravels postdate the

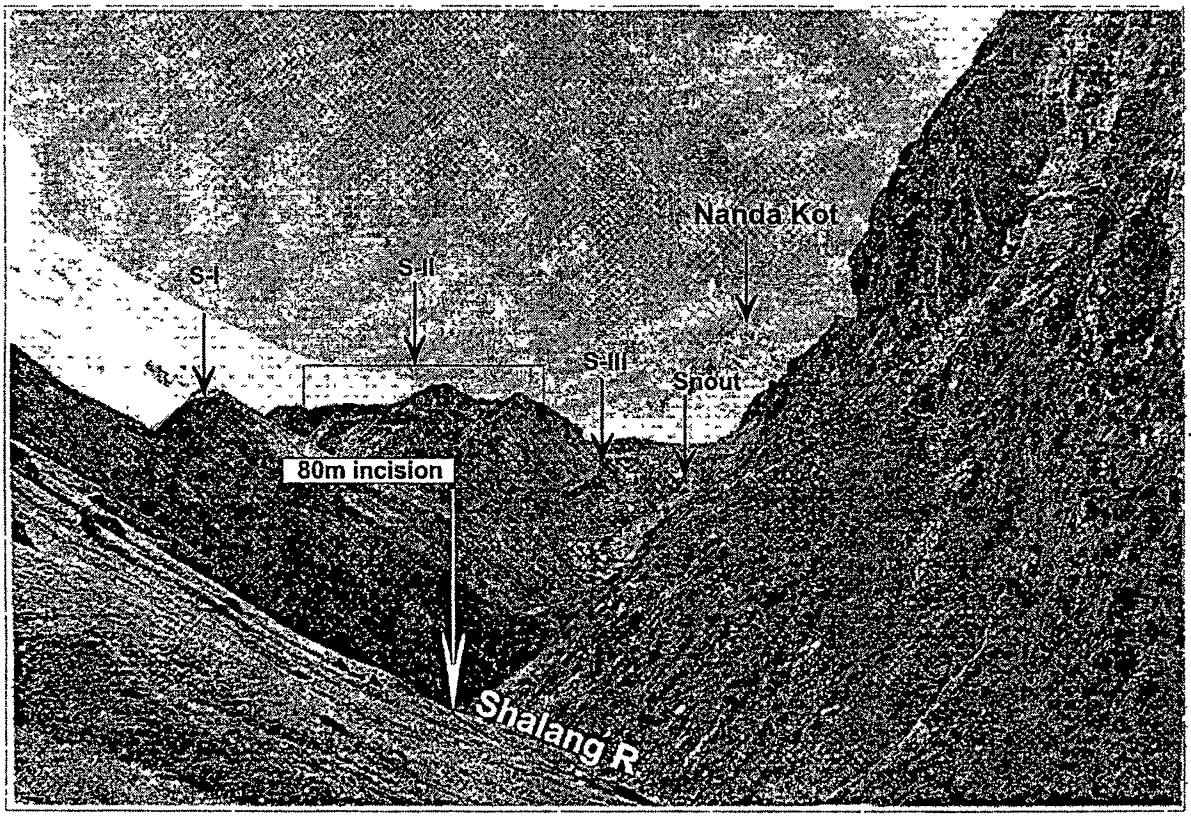

Figure-4.19. Field photograph of Shalang glacier (photo facing south). A preferential shift in Shalang glacier towards west (Nanda Kot) suggests relative movement along the basin with western flank being moved upwards compared to the eastern flank.

lacustrine sedimentation and suggest significant and abrupt increase in the meltwater discharge during deglaciation. Enhanced hydraulic discharge is an important component in the river bed incision. However, it alone could not have incised the outwash gravel.

Dhauli Ganga at Goting has transitional meandering-braided channel pattern (high width to depth ratio) and does not carry much energy (Fig. 4.20A). Such rivers leave much of its bed load along the course and are incapable of vertical incision (Holbrook and Schumm, 1999). In addition any gradual increase in valley slope, river can still maintain its gradient. It is only during events of drastic change in valley slopes a meandering river channel may braid with accompanying channel incision (Burnett and Schumm, 1983). Therefore, presence of four terraces with distinct vertical offsets suggests a contributary episodic tectonic component related with activity on the north-striking basin (east-west extension).

The truncated fault scree above the T_1 terrace having vertical offset of ~20 m with the succeeding one (T_2) indicate that it was generated along with the formation of terrace T1. Three subsequent events were of lesser magnitude (T_2 to T_4) in which displacement is <10 m (Fig. 4.20A and B). In addition to this no fresh scree association with these terraces is seen. This probably suggest that the succeeding events (T_2 to T_4) were caused by less intense seismic activity.

The IRSL chronology brackets the seismic events into two braod time range. Seismic event-1 is contrained between 24±3 to 18±3 ka at Goting and 20±3 to 17±2 ka at Garbayang whereas events-II, III and IV occurred between 14±2 and 13±2 ka. The single aliquot BGSL age of 11±1 ka obtained on outwash gravel (Terrace, T_1) at Goting suggests that incision postdate this age.

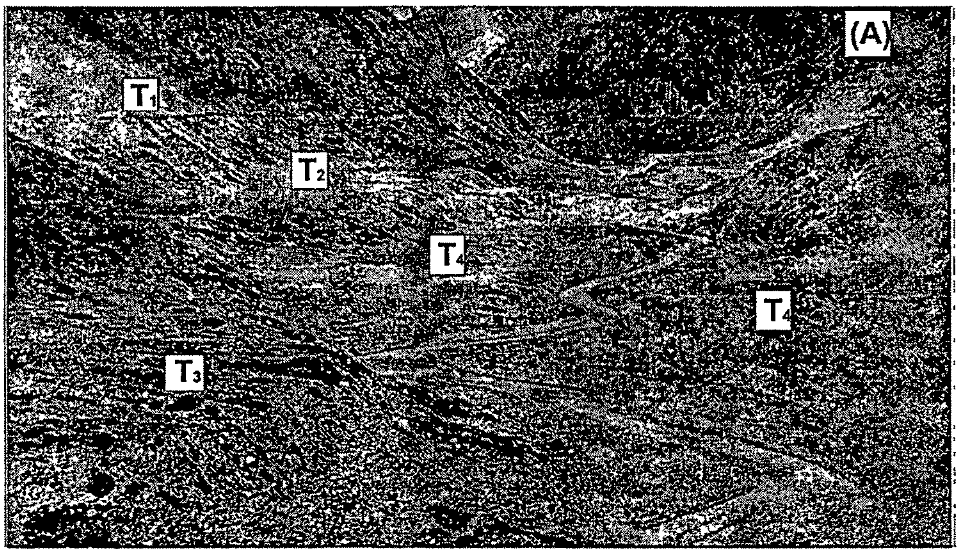

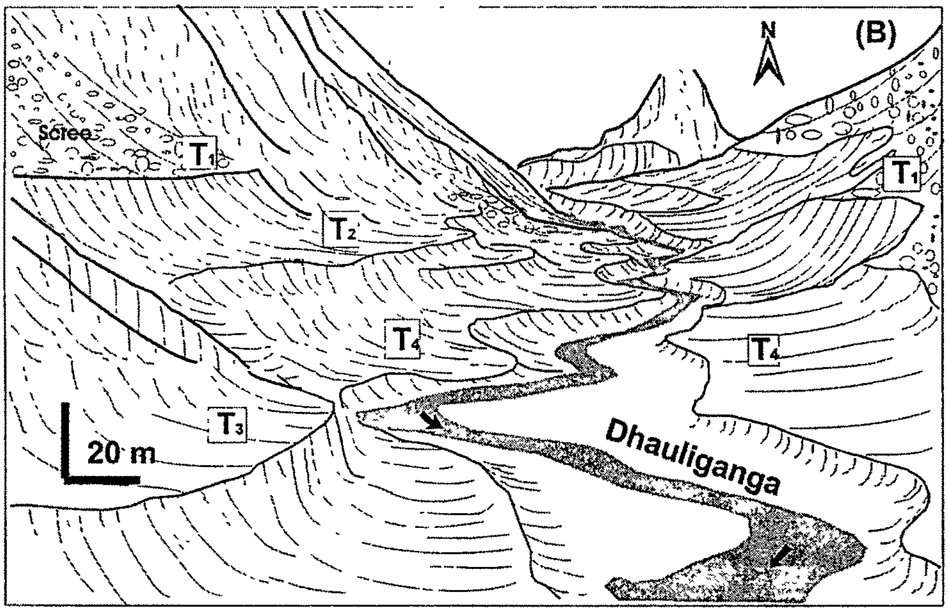

Figure-4.20. Four unpaired terrace developed on outwash gravel are located towards the southern end of the north trending rift valley at Goting. Each terrace separate from the succeeding one by distinct vertical off set suggesting episodic seismic activity